

In-situ neutron diffraction study of non-equilibrium phase transformation in advanced high-strength steels

Zhenzhen Yu, Zhili Feng, Ke An, Wei Zhang, Eliot D. Specht, Jian Chen, Xun-li Wang, and Stan David

Oak Ridge National Laboratory, Oak Ridge, TN, USA

Emails: yuz1@ornl.gov, fengz@ornl.gov, kean@ornl.gov, zhangw@ornl.gov, spected@ornl.gov, chenj2@ornl.gov, wangxl@ornl.gov, and davidsa1@ornl.gov

Abstract

The effect of heating rate on the phase transformation kinetics from ferrite (α) and martensite (α_M) to austenite (γ) in advanced high-strength steels (AHSS) was investigated. With the unique stroboscopic pump-probe neutron diffraction technique, a time-resolution of 0.1 second or less, corresponding to a time increment of 3°C or less, was achieved. A trend was clearly observed indicating that higher heating rate causes a wider and higher temperature range for the α to γ transformation. The lattice spacing change associated with the austenite formation on heating was obtained as well, which decreases at the early stage of transformation process and increases at the latter stage as a function of temperature. The kinetics governing such observed non-equilibrium phase transformation phenomena is discussed.

Keywords

Phase transformation, AHSS steels, neutron diffraction, martensite, ferrite.

Introduction

Advanced high-strength steels (AHSS) are an integral part of the materials solution for automotive industry to produce highly crash-resistant body structures while reducing the vehicle weight for fuel efficiency. The making of nearly all types of AHSS relies on carefully designed thermo-mechanically controlled processing (TMCP) route to achieve the target properties [1, 2]. The TMCP route often involves multiple steps of fast heating and cooling. Therefore, phase transformations under far-from-equilibrium conditions play an important role in the making of AHSS. The non-equilibrium phase transformation is also commonly associated with welding and other thermo-mechanical manufacturing processing of AHSS, which can lead to unexpected property degradation of the final fabricated structures/components [3-7]. However, our knowledge of non-equilibrium phase transformation is very limited in a complex alloy system during fast heating and cooling conditions. This is largely due to the lack of direct experimental measurement techniques to identify and quantify the transformation process. In this work, a novel asynchronous stroboscopic neutron diffraction experimental approach was designed and utilized to probe the non-equilibrium allotropic phase transformations of AHSS

during fast heating and cooling conditions with sub-second resolution. The information obtained from the in-situ measurement is essential to both the current generation AHSS and the development of the third generation AHSS for lightweight automotive applications.

Experimental Procedures

Two materials were used in this study, DR210 and DP980 steels. Their nominal chemical composition in mass percentage is listed in Table 1. For optical microscopy, the base metals were polished and etched in 4% picric-10% HCl-ethanol. Based on the optical microscopic examination, DR210 has predominately ferrite phase, as shown in Figure 1 (a). DP980 has a dual phase structure, i.e., ferrite (bcc) and martensite (bct) phases, as illustrated by the optical micrograph in Figure 1 (b), where darker color phase is martensite (determined from nano-hardness indentation measurement).

Table 1 Nominal chemical composition in mass percentage (wt%) of different AHSS.

Material	C	Mn	Cr	Si	Al	Cu
DR210	0.04	0.35	0.02	0.04	0.06	0.02
DP980	0.15	1.32	0.03	0.32	0.04	0.02

Due to the deep penetration capability of neutron (of the order of centimeters), in-situ neutron diffraction technique was utilized for “bulk” volume-averaged measurement of phase transformation phenomenon in the two steels. The measurement was performed at the VULCAN beam line of spallation neutron source (SNS) at Oak Ridge National Laboratory (ORNL) [8]. An electric resistance-heating device was built to heat the sample. The samples were heated up to 1050°C under controlled rates of 3°C/s and 30°C/s, respectively, and then cool down freely to room temperature in argon gas atmosphere.

In order to capture the phase transformation under fast heating conditions, sub-second time resolution is desired for the in-situ experiment. To achieve such requirement of in-situ and time-resolved measurement, the experiment was specially designed following three steps: (1) maximize the diffraction volume to increase the intensity of diffraction pattern; (2) minimize the temperature gradient within the diffraction volume to maintain measurement accuracy; (3) superimpose diffraction patterns of

repeating thermal cycles to enhance the diffraction intensity with the aid of a stroboscopic pump-probe technique.

First of all, the maximum slit size for neutron diffraction was used to provide a large diffraction volume with a length of 17mm at the center of the sample. It allows more neutrons to be diffracted per unit time, and thus improves the time resolution. Secondly, to obtain a relatively uniform temperature distribution within the diffraction volume, the specimen's geometry and dimensions were optimized by means of transient electrical-thermal finite element modeling. The optimized sample dimensions were 2mm in thickness, 8mm in width, and 240mm in length. For slow heating case (3°C/s), notches were made near the ends of the sample, to increase the local heat generation while restricting heat loss to the fixtures. Additionally, the temperature uniformity were experimentally verified with three thermocouples attached on the sample surface, 5mm apart from each other along the length direction, to record the temperature distribution and gradient at the center of the sample. Finally, a unique stroboscopic pump-probe technique [9, 10] was used, that tracks and stores data information of every single neutron separately. It allows for superimposition of the diffraction patterns from repeats of the heating-cooling cycle, leading to enhanced intensity of the diffraction peaks. In other words, the diffraction pattern intensity was enhanced by repeating the heating-cooling cycles in each sample, which makes the sub-second resolution measurement of non-equilibrium phase transformation feasible. Rietveld method [11-13] was used to fit the full diffraction pattern to obtain the information such as lattice spacing evolution and phase fractions during the thermal process.

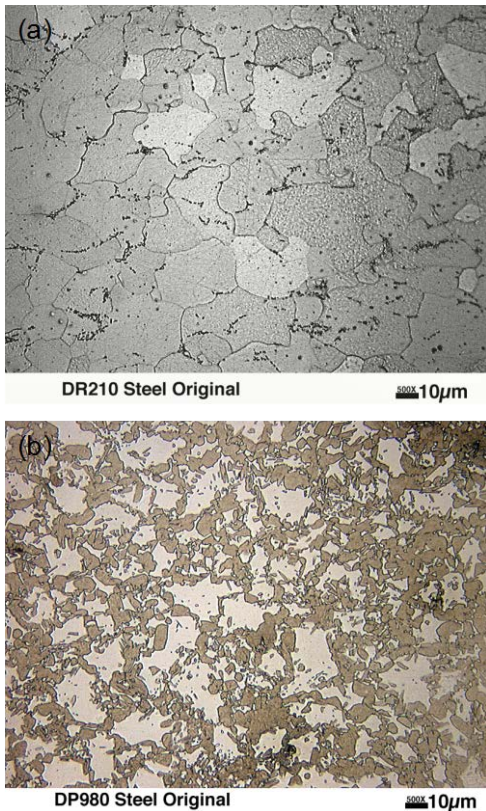


Fig. 1 Light optical micrographs of (a) DR210, and (b) DP980 steels. In (b), darker color represents martensite phase.

Results and Discussion

Based on the temperature records from thermocouples, the temperature gradients within the diffraction volume of samples are less than 3°C during the heating and cooling process.

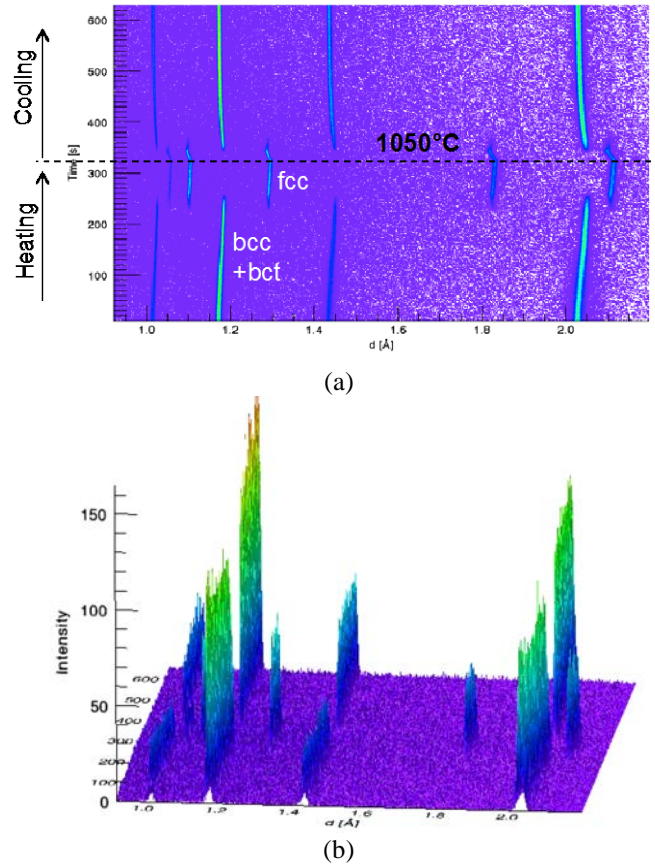


Fig.2 Neutron diffraction pattern as a function of time in DP980 reveals the phase transformation process in (a) 2D and (b) 3D views, respectively. The heating rate is 3°C/s.

Figure 2 shows the evolution of diffraction patterns in DP980 in a complete heating and cooling cycle, and the heating rate is 3°C/s. The black dashed horizontal line in Figure 2(a) separates the heating and cooling processes. Note that in Figure 2, peak pattern of martensite (bct, α_M) phase cannot be distinguished from that of ferrite (bcc, α), since the lattice parameters of α and α_M are fairly close [14]. As temperature increases during heating, austenite (fcc, γ) phase starts to form and eventually replaces the original phases. The opposite is observed as the temperature decreases during the cooling process. Note that in Figure 2 (a), before the maximum temperature of 1050°C is reached; there is a gradual increase in d spacing as a function of temperature, and the opposite during cooling. Similar phase transformation processes are observed in DR210 and DP980 samples with different heating rates. Figures 3 and 4 reveal more details of the phase transformation processes during heating obtained from the neutron diffraction experiment.

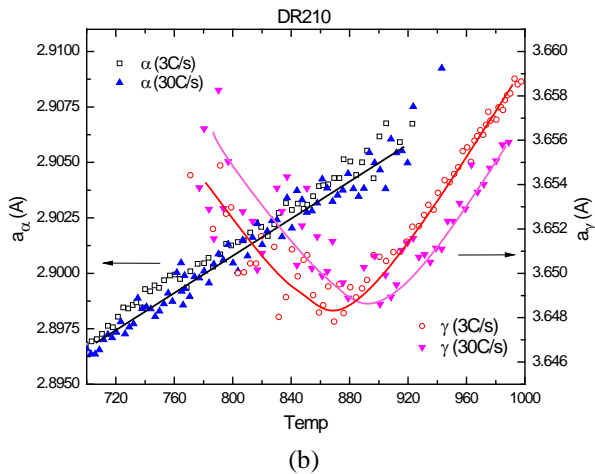
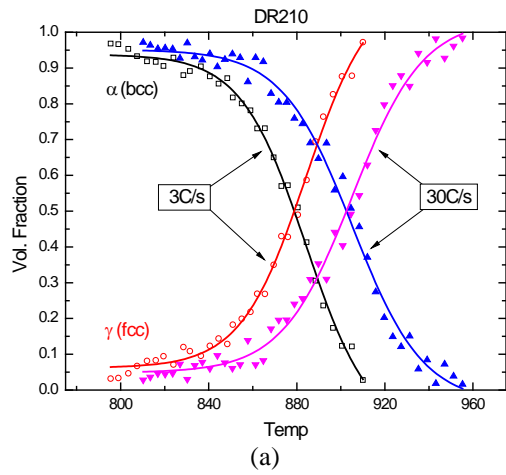


Fig. 3 Phase transformation from ferrite (α) to austenite (γ) in DR210: variations of their (a) volume fractions and (b) lattice parameters as a function of temperature ($^{\circ}\text{C}$).

In DR210, as shown in Figure 3 (a), the heating rate does not affect the initiation of phase transformation significantly, but largely widens the phase transformation temperature range. Table 2 summarizes the temperature range (ΔT) for the completion of phase transformation process. For DR210, it changes from 114°C to 141°C , as the heating rate increases from 3°C/s to 30°C/s . Note that the newly formed austenite phase at the very beginning of phase transformation process generates peaks with fairly low intensity in the diffraction pattern. Especially for the 30°C/s case, Rietveld refinement may not be able to fit the peaks diffracted from austenite phase with a volume fraction lower than 3%. Same difficulties are encountered when fitting the remaining fraction of ferrite phase (e.g., $<3\%$ volume fraction) at the ending of transformation process. Therefore, for the purpose of reasonable comparison among different cases, in Table 2, the initiation of phase transformation temperature was defined as $\sim 3\%$ volume fraction of austenite was formed, and the completion corresponds to the temperature as $\sim 97\%$ of austenite was present in the material. Figure 3 (b) shows the change of lattice parameters in ferrite (a_{α}) and austenite (a_{γ}) as a function of temperature. a_{α} almost increases linearly as temperature rises due to thermal expansion. However, a_{γ} firstly decreases as temperature increases, until $\sim 50\%$ volume fraction of austenite was formed. Afterwards, a_{γ} increases with the temperature. The unusual lattice parameter change is

possibly associated with the microscopic heterogeneity of alloying elements (e.g., carbon concentration) during phase transformation. Austenite prefers a carbon-rich site to nucleate [15, 16]. Therefore, it is expected that the “average” carbon concentration in the newly formed austenite would decrease as more austenite forms upon heating. This leads to the initial decrease in the d-spacing of austenite.

Table 2 Initiation and completion temperature of α to γ phase transformation process in DR210 and DP980 at different heating rates.

Sample	$\sim 3\% \gamma$ ($^{\circ}\text{C}$)	$\sim 97\% \gamma$ ($^{\circ}\text{C}$)	ΔT ($^{\circ}\text{C}$)
DR210 3°C/s	796	910	114
DR210 30°C/s	810	951	141
DP980 3°C/s	724	846	122
DP980 30°C/s	747	884	137

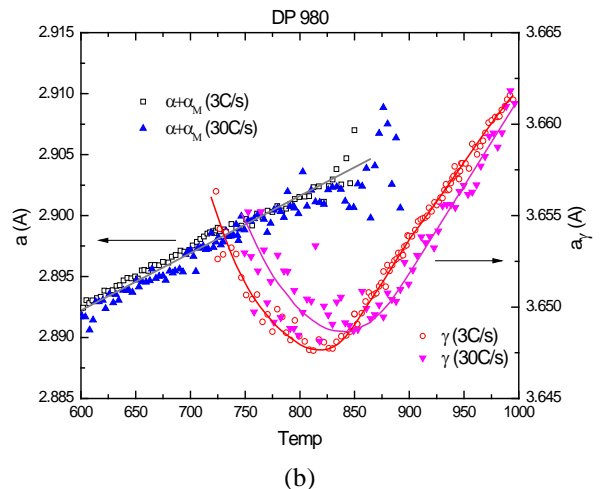
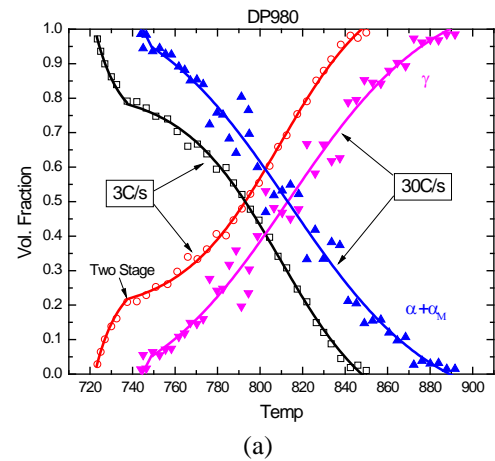


Fig.4 Phase transformation from ferrite (α) + martensite (α_M) to austenite (γ) in DP980: variations of their (a) volume fractions and (b) lattice parameters as a function of temperature ($^{\circ}\text{C}$).

For DP980, Figure 4(a) and Table 2 indicates as heating rate increases, the phase transformation process shifts to a higher temperature range. Both the initiation and completion of the phase transformation process was shifted to higher

temperature level due to the increased heating rate in DP980. As listed in Table 2, the temperature range (ΔT) for the completion of phase transformation process in DP980 changes from 122°C to 137°C, as the heating rate increases from 3°C/s to 30°C/s. Compared to DR210, phase transformation in DP980 initiates and completes at much lower temperatures. Note that in Figure 4 (a), for 3°C/s heating only, a two-stage phase transformation was observed. For phase transformation at 30°C/s, such behavior is not as obvious. The mechanisms of such difference due to heating rate are being investigated. Compared to DP980, carbon in mass percentage in DR210 is much lower, and the two-stage phase transformation was not observed.

Conclusions

Influence of heating rates on the non-equilibrium phase transformation kinetics in advanced high-strength steels was studied by in-situ neutron diffraction experiments. With the newly developed stroboscopic pump-probe technique and data collection procedure, a sub-second time resolution was achieved, allowing capturing the phase transformation process with sufficient resolution at fast heating conditions. In both DP980 and DR210, increasing heating rate causes the temperature range for ferrite/martensite to austenite transformation shifting to higher values. For DP980, which has higher carbon concentration, a two-stage phase transformation process was observed under the slow heating rate condition. Last but not the least, unique d-spacing changes were observed. It is possibly related to the carbon concentration changes in the newly formed austenite, which depends upon the kinetics of phase transformation.

Acknowledgments

This research was financially supported by the Laboratory Directed Research and Development (LDRD) program at Oak Ridge National Laboratory (ORNL). This work was also benefited from the use of ORNL's Spallation Neutron Source (SNS), which is sponsored by the Scientific User Facilities Division, Office of Basic Energy Sciences, U.S. Department of Energy.

References

[1] A.S. Podder, I. Lonardelli, A. Molinari, H.K.D.H. Bhadeshia, "Thermal stability of retained austenite in bainitic steel: an in situ study", *Proceedings of the Royal Society a-Mathematical Physical and Engineering Sciences*, 467 (2011), pp. 3141-3156.
[2] R.R. Mohanty, O.A. Girina, N.M. Fonstein, "Effect of Heating Rate on the Austenite Formation in Low-Carbon High-Strength Steels Annealed in the Intercritical Region", *Metall Mater Trans A*, 42A (2011), pp. 3680-3690.
[3] N. Sreenivasan, M. Xia, S. Lawson, Y. Zhou, "Effect of laser welding on formability of DP980 steel", *J Eng Mater-T Asme*, 130 (2008), pp. -.
[4] X. Sun, E.V. Stephens, M.A. Khaleel, "Effects of fusion zone size and failure mode on peak load and energy

absorption of advanced high strength steel spot welds under lap shear loading conditions", *Eng Fail Anal*, 15 (2008), pp. 356-367.
[5] J.E. Gould, S.P. Khurana, T. Li, "Predictions of microstructures when welding automotive advanced high-strength steels - A combination of thermal and microstructural modeling can be used to estimate performance of welds in advanced high-strength steels", *Welding Journal*, 85 (2006), pp. 111S-116S.
[6] M.I. Khan, M.L. Kuntz, Y. Zhou, "Effects of weld microstructure on static and impact performance of resistance spot welded joints in advanced high strength steels", *Sci Technol Weld Joi*, 13 (2008), pp. 294-304.
[7] Z. Feng, *Weldability and Performance of Advanced High-Strength Steels (AHSS) in Automotive Structure*, in: SAE World Congress, Detroit, MI, USA, 2007.
[8] X.L. Wang, T.M. Holden, G.Q. Rennich, A.D. Stoica, P.K. Liaw, H. Choo, C.R. Hubbard, "VULCAN - The engineering diffractometer at the SNS", *Physica B-Condensed Matter*, 385 (2006), pp. 673-675.
[9] M.R. Daymond, P.J. Withers, "A new stroboscopic neutron diffraction method for monitoring materials subjected to cyclic loads: Thermal cycling of metal matrix composites", *Scripta Mater*, 35 (1996), pp. 717-720.
[10] T.C. Hansen, "Future trends in high intensity neutron powder diffraction", *European Powder Diffraction Epdic*, 8, 443-4 (2004), pp. 181-186.
[11] R.B. Vondreele, J.D. Jorgensen, C.G. Windsor, "Rietveld Refinement with Spallation Neutron Powder Diffraction Data", *J Appl Crystallogr*, 15 (1982), pp. 581-589.
[12] R.J. Hill, C.J. Howard, "Quantitative Phase-Analysis from Neutron Powder Diffraction Data Using the Rietveld Method", *J Appl Crystallogr*, 20 (1987), pp. 467-474.
[13] X.L. Wang, J.A. Fernandezbaca, C.R. Hubbard, K.B. Alexander, P.F. Becher, "Transformation Behavior in Al₂O₃-ZrO₂ Ceramic Composites", *Physica B*, 213 (1995), pp. 824-826.
[14] N. Jia, Z.H. Cong, X. Sun, S. Cheng, Z.H. Nie, Y. Ren, P.K. Liaw, Y.D. Wang, "An in situ high-energy X-ray diffraction study of micromechanical behavior of multiple phases in advanced high-strength steels", *Acta Mater*, 57 (2009), pp. 3965-3977.
[15] S.W. Thompson, G.S. Farr, P.R. Howell, *Nucleation of Austenite During Intercritical Annealing of a Commercial Low-Alloy Steel*, in: A.R. Marder, J.I. Goldstein (Eds.) *Proceedings of an international conference on phase transformations in ferrous alloys*, The Metallurgical Society of AIME, Warrendale, Pennsylvania 15086, 1983, pp. 411.
[16] T.A. Palmer, J.W. Elmer, "Direct observations of the formation and growth of austenite from pearlite and allotriomorphic ferrite in a C-Mn steel arc weld", *Scripta Mater*, 53 (2005), pp. 535-540.
[17] Z. Yu, Z. Feng, K. An, W. Zhang, E.D. Specht, J. Chen, X.L. Wang, S. David, unpublished work, in, Oak Ridge National Laboratory, Oak Ridge, 2012.
[18] G.R. Speich, V.A. Demarest, R.L. Miller, "Formation of Austenite during Intercritical Annealing of Dual-Phase Steels", *Metallurgical Transactions a-Physical Metallurgy and Materials Science*, 12 (1981), pp. 1419-1428.